Published in final edited form as:
*Cell Rep*. 2012 December 27; 2(6): 1697–1709. doi:10.1016/j.celrep.2012.10.025.

# Epistasis between microRNAs 155 and 146a during T cell-mediated antitumor immunity

**Thomas B. Huffaker**[1,3], **Ruozhen Hu**[1,3], **Marah C. Runtsch**[1], **Erin Bake**[1], **Xinjian Chen**[1], **Jimmy Zhao**[2], **June L. Round**[1], **David Baltimore**[2], and **Ryan M. O'Connell**[1,*]

[1]Division of Microbiology and Immunology, Department of Pathology, University of Utah, 15 N. Medical Dr. East, JMRB, Salt Lake City, UT, 84112

[2]Division of Biology, California Institute of Technology, 330 Braun, 1200 E. California Blvd., Pasadena, CA 91125

## SUMMARY

An increased understanding of antitumor immunity is necessary to improve cell-based immunotherapies against human cancers. Here, we investigated the roles of two immune system-expressed microRNAs (miRNAs), miR-155 and miR-146a, in the regulation of antitumor immune responses. Our results indicate that miR-155 promotes and miR-146a inhibits IFNγ responses by T cells and reduced solid tumor growth *in vivo*. Using a novel double knockout (DKO) mouse strain deficient in both miR-155 and miR-146a, we have also identified an epistatic relationship between these two miRNAs. DKO mice had defective T cell responses and tumor growth phenotypes similar to *miR-155*−/− mice. Further analysis of the T cell compartment revealed that miR-155 modulates IFNγ expression through a mechanism involving repression of Ship1. Our work reveals critical roles for miRNAs in the reciprocal regulation of CD4+ and CD8+ T cell-mediated antitumor immunity, and demonstrates the dominant nature of miR-155 during its promotion of immune responses.

## INTRODUCTION

Combating solid tumors remains an enormous challenge for the biomedical community. The need for improved therapies beyond radiation and chemotherapy has become evident, and there is growing interest in optimizing the use of immunotherapy as a treatment option. Among the cell types that hold promising therapeutic potential are T lymphocytes, including CD4+ IFNγ-expressing Th1 cells and cytotoxic CD8+ T cells, which elicit tumor antigen specific responses to direct the tumor microenvironment in a manner that restricts or eliminates tumor growth (Dougan and Dranoff, 2008; Dunn et al., 2004; Shiao et al., 2011). However, there remain several aspects of antitumor immunity that are unclear and appear to be governed by complex regulatory systems that have limited this application in the clinic thus far (Zitvogel et al., 2006). Therefore, an improved understanding of the molecular networks that influence T lymphocyte biology in the context of antitumor responses is



*Direct all correspondence to: Ryan M. O'Connell (ryan.oconnell@path.utah.edu) phone: (801) 213-4153 .
[3]Equal contribution



The authors have no financial conflicts of interests except for David Baltimore, who is a consultant for Regulus Therapeutics.

needed, and this has the potential to improve our ability to manipulate this response in a manner that promotes tumor rejection.

Mammalian miRNAs have recently emerged as important regulators of immune cell development and function, and represent a novel layer of control over cellular physiology (O'Connell et al., 2010c). miRNAs are encoded by the genome and their transcription is regulated in a manner similar to other inflammatory protein coding genes, and this can involve such factors as NF-κB and AP-1 (O'Connell et al., 2007; Taganov et al., 2006; Thai et al., 2007). Following their biogenesis, miRNAs are loaded into RISC and guide this complex to the 3′ untranslated regions (UTRs) of key target genes resulting in repressed expression (Filipowicz et al., 2008). In recent years, specific miRNAs have been implicated in the regulation of inflammatory T cell biology where they can dramatically impact autoimmune and antimicrobial responses in mammals (Lu et al., 2009; O'Connell et al., 2010b; Rodriguez et al., 2007; Thai et al., 2007).

One of the most prominent miRNAs linked to inflammation is miR-155, which is upregulated in both myeloid and lymphoid cells following their activation (Haasch et al., 2002; O'Connell et al., 2007). In the T cell compartment, miR-155 regulates T regulatory cell fitness through a mechanism involving Socs1 repression (Lu et al., 2009), while also being required for the development of inflammatory Th17 cells during autoimmunity driven by specific tissue antigens (Murugaiyan et al., 2011; O'Connell et al., 2010b). miR-155 has been shown to be necessary for effective vaccination against *S. typhimurium* and immunity against *H. pylori* (Oertli et al., 2011; Rodriguez et al., 2007). In contrast to miR-155, miR-146a limits T cell activation and promotes resolution of inflammatory responses. *miR-146a*−/− mice develop spontaneous autoimmunity and cancer upon aging, and this phenotype involves, among other things, hyperactivation of T cells via de-repression of its targets Irak1 and Traf6 (Boldin et al., 2011b; Yang et al., 2012; Zhao et al., 2011). Stat1 has also been shown to be a functionally relevant target of *miR-146a*−/− in Treg cells (Lu et al., 2010). Thus, these two miRNAs appear to have opposite impacts on inflammatory responses carried out by T lymphocytes in the contexts of autoimmunity and infection.

To date, little is known about the roles of T cell-expressed miR-155 and miR-146a during antitumor immune responses. To address this, we first tested the ability of miR-155 to mediate antitumor immunity using multiple models of syngeneic solid tumor growth in mice. We found that *miR-155*−/− mice permit enhanced growth of transplanted EL4-luc lymphoma and B16 melanoma cells compared to Wt controls. This was accompanied by a cell intrinsic defect in IFNγ-expressing T cells in tumor bearing mice. In contrast to *miR-155*−/− mice, *miR-146a*−/− mice suppressed tumor growth compared to Wt controls, and this correlated with an elevated IFNγ response. Interestingly, mice deficient in both miR-155 and miR-146a, or DKO mice, had IFNγ responses resembling those observed in *miR-155*−/− mice *in vivo*. Mechanistically, we found that miR-155 regulates CD4+ T cell expression of IFNγ through a process involving repression of Ship1. These findings reveal that miRNAs are instrumental in directing CD4+ and CD8+ T cell-mediated antitumor responses, and that miR-155 plays a dominant role compared to miR-146a in the promotion of IFNγ-expressing T cell development in this context.

## RESULTS

### Enhanced growth of syngeneic tumors in *miR*-155−/− mice

To assess the impact of miR-155 on solid tumor growth, we administered $2\times10^6$ syngeneic EL4-luc lymphoma cells subcutaneously into Wt or *miR-155*−/− mice and monitored tumor growth over a time course. Although the tumor sizes were similar between the groups by day 9 post-injection, substantial differences in tumor diameters and weights were observed

by day 12, with tumors growing much larger in *miR-155*−/− versus Wt mice (Figure 1A and 1B). Because the tumor cells express luciferase, we also found that luciferase activity correlated with tumor size using Xenogen whole animal imaging (Figure 1C and Figure S1). Of note, we did not observe a luciferase signal from locations other than the site of tumor injection, suggesting that the tumor cells had not metastasized. Next, we challenged both groups of mice with two other types of syngeneic tumors, B16-F1 or B16-F10 melanoma cells, and once again observed increased tumor growth in *miR-155*−/− versus Wt mice (Figure 1D, 1E and 1F). Of note, the differences in B16 tumor growth between the genotypes were not as dramatic as those observed with the EL4-luc tumors, likely a consequence of differences in tumor immunogenicity.

H&E stained tumor tissue sections revealed significant necrosis in tumors growing in Wt mice, while those growing in *miR-155*−/− mice had few of these features (Figure 1G). Furthermore, we observed elevated numbers of TILs in both EL4-luc and B16-F10 tumors growing in Wt compared to *miR-155*−/− hosts (Figure 1G and 1H). These observations indicate that *miR-155*−/− mice have a defect in limiting syngeneic tumor growth, and this correlates with a defective antitumor immune response.

## Defective IFNγ+CD4+ T cell development in *miR*-155−/− tumor bearing mice occurring through a CD4+ T cell intrinsic mechanism

miR-155 is expressed predominately in the immune system following cellular activation, and has been implicated in directing antigen specific responses and lineage skewing by lymphocytes *in vivo*. Because IFNγ-expressing T cells are instrumental in repressing tumor growth (Ikeda et al., 2002; Jiang et al., 2011; Maekawa et al., 1988; Muranski et al., 2011; Yim et al., 1999), we assayed the amount of CD4+ IFNγ-expressing T cells in Wt compared to *miR-155*−/− tumor bearing mice. In both the spleens and lymph nodes of mice with EL4-luc tumors, a lack of miR-155 led to significant reductions in both the percentage and absolute number of IFNγ producing CD4+ T cells compared to Wt controls (Figure 2A and 2B, and Figure S2). Of note, we only observed significant differences in the total number of IFNγ+CD4+ splenic T cells in Wt versus *miR-155*−/− mice after administration of the tumor (Figure 2C). Further demonstrating a defective tumor immune response, we found that transfer of total splenocytes from Wt, but not *miR-155*−/−, tumor-bearing mice protected naïve Wt mice from a primary tumor challenge (Figure S3).

Next, we wanted to determine if this defective CD4+ T cell response was due to cell intrinsic or extrinsic pathways regulated by miR-155. To make this assessment, $4\times10^6$ naïve *miR-155*−/− or Wt CD45.2+ CD4+ T cells were transferred into sub-lethally irradiated CD45.1+ Wt recipients and $5\times10^5$ B16-F10 tumor cells injected the next day. Consistent with miR-155 playing a CD4+ T cell intrinsic role, the transferred CD45.2+ *miR-155*−/− CD4+ T cells exhibited defective IFNγ responses compared to CD45.2+ Wt CD4+ T cells in the tumors of CD45.1+ Wt recipient mice (Figure 2D and 2E). To corroborate these findings, the reverse experiment was performed by adoptively transferring $4\times10^6$ naïve CD45.1+ CD4+ Wt T cells into sub-lethally irradiated CD45.2+ Wt or *miR-155*−/− mice one day before challenging these mice with B16-F10 cells. Another group of CD45.2+ *miR-155*−/− mice received $4\times10^6$ naïve CD45.2+ *miR-155*−/− CD4+ T cells following irradiation, and served as a control group. The transferred Wt T cells readily differentiated into IFNγ-expressing cells both in the spleens (Figure 2F, 2G and 2H) and the tumors (Figure 2F and 2I) of *miR-155*−/− mice. This significantly increased the percentage of IFNγ expressing cells within the tumors, but did not reach Wt levels (Figure 2j). Furthermore, tumors in *miR-155*−/− mice having received Wt CD4+ T cells trended towards being smaller than tumors growing in *miR-155*−/− mice that received miR-155−/− CD4+ T cells (Figure 2K). Cellular engraftment and IFNγ+CD4+ T cell differentiation (by the transferred Wt T cells) was more robust in *miR-155*−/− versus Wt recipients (Figure 2F, 2G and 2H),

possibly due to an increased availability of T cell niches in mice lacking miR-155. These findings, and similar observations with EL4-luc tumor cells (Figure S3), indicate that miR-155 plays a cell intrinsic role during the formation of IFNγ-expressing CD4+ T cells in response to solid tumor growth.

## miR-155 is required for accumulation of IFNγ+CD8+ T cells in tumors, and this also occurs through a CD8+ T cell intrinsic mechanism

The immune response against solid tumors involves multiple cell types, including both CD4+ and CD8+ T cells. Although we have found a clear T cell intrinsic function for miR-155 in the promotion of IFNγ responses by CD4+ T cells in response to solid tumors, a role for miR-155 in CD8+ T cell biology during antitumor immunity has not been reported. Thus, we first examined IFNγ expression by CD8+ T cells following their activation *in vitro*, and observed defective IFNγ mRNA levels in the absence of miR-155 (Figure 3A). Next, we assessed the CD8+ TIL population in tumors growing in Wt versus *miR-155*−/− mice, and observed a significant reduction in the percentage of IFNγ+CD8+ T cells among total CD8+ T cells in the absence of miR-155 (Figure 3B). Adoptively transferred *miR-155*−/− CD45.2+ CD8+ T cells were significantly defective in accumulating and producing IFNγ in tumors growing in CD45.1+ Wt mice, indicating a cell intrinsic role for miR-155 in CD8+ T cells (Figure 3C). Further supporting a CD8+ T cell intrinsic role for miR-155, transfer of Wt CD45.1+CD8+ T cells into sub-lethally irradiated CD45.2+ Wt or *miR-155*−/− hosts followed by a tumor challenge revealed that Wt CD8+ T cells could still mediate strong IFNγ responses in a *miR-155*−/− environment (Figure 3D and 3E). *miR-155*−/− mice receiving Wt CD8+ T cells also tended to have reduced tumor weights than those receiving *miR-155*−/− CD8+ T cells (Figure 3E). Thus, miR-155 functions within both CD4+ and CD8+ T cells to promote IFNγ-dependent antitumor immunity.

## miR-155 plays a dominant role compared to miR-146a during T cell-mediated tumor immunity

Like miR-155, miR-146a is also expressed in activated T cells. However, in contrast to miR-155, *miR-146a*−/− T cells have been reported to be hyper-activated during acute and chronic immune responses (Yang et al., 2012). Therefore, we tested whether *miR-146a*−/− mice have enhanced antitumor immunity compared to Wt mice. *miR-146a*−/−, *miR-155*−/− and Wt mice were inoculated s.c. with $1\times10^6$ B16-F10 cells and tumor growth was monitored over a time course (Figure 4A). Interestingly, tumors grew at a reduced rate in the absence of miR-146a compared to Wt mice, while once again they grew larger in *miR-155*−/− mice, suggesting that these miRNAs play opposing roles during antitumor responses.

To examine the cross-regulation of tumor immunity by miR-155 and miR-146a, we created mice deficient in both miRNAs (Figure 4B). Using these mice, we assessed whether these opposing phenotypes would be canceled out, or if one of these two miRNAs plays a dominant role. Double knockout (DKO) mice were viable and fertile and did not exhibit obvious gross abnormalities by the age of 8 weeks. The absence of both miR-155 and miR-146a expression was confirmed by qPCR using RNA from *in vitro* activated CD4+ T cells (Figure 4C). When these mice and the relevant control groups were challenged with $1\times10^6$ B16-F10 tumor cells, there was a consistent trend towards increased tumor growth in DKO compared to Wt mice, similar to tumors growing in *miR-155*−/− mice (Figure 4D and 4E). Again, *miR-146a*−/− mice restricted tumor growth compared to Wt mice.

IFNγ+CD4+ T cell numbers in the spleens of both DKO and *miR-155*−/− tumor bearing mice were significantly reduced compared to Wt mice, while *miR-146a*−/− mice had the highest levels (Figure 4F). This same trend was also observed when CD45.2+ Wt, *miR-155*−/−, *miR-146a*−/− or DKO CD4+ T cells were transferred into CD45.1+ Wt mice

followed by 15 days of tumor growth, consistent with these miRNAs playing CD4+ T cell intrinsic roles to regulate IFNγ production (Figure 4G and 4H).

Upon analyzing single cell tumor suspensions by FACS, miR-155−/− and DKO mice had reduced percentages of cells in the FSC-SSC leukocyte gate versus those observed in Wt mice, and this cellular compartment contained CD3+CD4+ and CD3+ CD8+ TILs (Figure 5A). Alternatively, increased percentages of TILs were observed in tumors from *miR-146a*−/− compared to Wt mice (Figure 5A). The percentages of IFNγ+CD4+ and IFNγ+CD8+ T cells among total CD4+ or CD8+ TILs, respectively, were reduced in tumors growing in *miR-155*−/− and DKO mice, and marginally increased in tumors from *miR-146a*−/− animals (Figure 5B and 5C). Upon FACS sorting CD3+CD4+ or CD3+CD8+ TILs from the tumors, we recovered fewer numbers of total and IFNγ+CD4+ and IFNγ+CD8+ T cells from tumors growing in *miR-155*−/− and DKO mice compared to Wt mice, while *miR-146a*−/− mice had elevated amounts (Figure 5D and 5E). Furthermore, miR-155 and miR-146a were expressed in both CD4+ and CD8+ TILs (Figure S4). Together, these observations indicate that miR-155 plays dominant, T cell-intrinsic roles in promoting antitumor responses by both CD4+ and CD8+ T cells.

## miR-155 targets the IFNγ regulator Ship1 in T cells

Because we found that miR-155 functions in CD4+ T cells during the antitumor response, we FACS sorted CD4+ T cells from the spleens of *miR-155*−/− and Wt tumor bearing mice and analyzed gene expression differences to obtain mechanistic insight into its impact on IFNγ expression. De-repression of *Ship1*, a previously identified target of miR-155 in myeloid cells (O'Connell et al., 2009), was observed by qPCR in cells lacking miR-155 (Figure 5A). BIC, the noncoding RNA that produces miR-155, was assays as a control and not detected in *miR-155*−/− cells. To assay Ship1 expression at the protein level in *miR-155*−/− CD4+ T cells, Western blotting was performed using lysates prepared from naïve Wt or *miR-155*−/− T cells that had been activated with αCD3 and αCD28 antibodies for 96 hours (Figure 5B). Elevated Ship1 protein concentrations were observed in *miR-155*−/− T cells under these conditions. Next, we extended our analysis to activated DKO CD4+ T cells and again found enhanced expression of Ship1 at the protein and mRNA levels in both *miR-155*−/− and DKO CD4+ T cells compared to Wt and *miR-146a*−/− cells (Figure 5C and 5D). Importantly, levels of Ship1 inversely correlated with the expression of IFNγ in Wt, *miR-155*−/− and DKO T cells (Figure 5E). Of note, there was little impact by the different miRNA deficiencies on CD4+ T cell growth *in vitro* (Figure S5), and activated *miR-146a*−/− CD4+ T cells still produced elevated levels of IFNγ even after CD25+ Tregs were depleted (Figure S6).

To test the functional impact of elevated Ship1 expression (as observed in the absence of miR-155) on IFNγ levels, we utilized shRNAs to knockdown Ship1 expression in activated Wt, *miR-155*−/−, *miR-146a*−/− or DKO CD4+ T cells. We found that in T cells of all genotypes tested, reductions in *Ship1* using either of two different shRNAs resulted in increased expression of *IFNγ* mRNA compared to cells given a scrambled control vector (Figure 5F). Knockdown by the shRNA was confirmed by Western blotting against Ship1 (Figure 5G). Expression of a Ship1 shRNA in activated CD4+ T cells also increased production of IFNγ at the protein level as determined by ELISA (Figure 5H). Retroviral transduction of CD4+ T cells was approximately 50% in all cases as determined by FACS to identify GFP+ cells. Next, we also assayed Ship1 protein levels in CD8+ T cells from the different groups. Like CD4+ T cells, Ship1 was also elevated in *miR-155*−/− and DKO compared to Wt and *miR-146a*−/− CD8+ T cells (Figure 6I). Taken together, these findings indicate that Ship1 is repressed by miR-155 in both CD4+ and CD8+ T cells. Furthermore, miR-155 promotes IFNγ expression by CD4+ T cells through a mechanism involving

repression of Ship1. However, the partial recovery of the IFNγ phenotype following Ship1 knockdown indicates that addition targets of miR-155 are also involved in this phenotype.

## DISCUSSION

MicroRNA-155 has quickly emerged as an important promoter of inflammatory responses, with a clear connection to autoimmunity. Furthermore, miR-155 is overexpressed in a variety of tumor cell types and can promote tumor growth in many cases (Bakirtzi et al., 2011; Chang et al., 2011; Han et al., 2012; Philippidou et al., 2010; Segura et al., 2010; Volinia et al., 2006; Zheng et al., 2012). Thus, it has been suggested that therapeutic inhibition of miR-155 may be a strategic means to treat autoimmunity or cancer. However, in the current study, we found that transferred syngeneic tumors grew substantially larger in mice genetically deficient in miR-155. Despite the tumors being weakly immunogenic, defects in the antitumor immune response were observed in the absence of miR-155 demonstrating a protective role for this miRNA in immune cells in the context of a tumor challenge. Consequently, clinical approaches aimed at targeting miR-155 within tumor cells themselves could have deleterious consequences if unintended repression of miR-155 occurs in immune cells. One could imagine this to be highly possible because solid tumors are physically associated with TILs. Furthermore, inhibition of miR-155 to treat autoimmunity might also block protective functions mediated by miR-155, including tumor immunosurveillance. Thus, our results clearly indicate the need for highly specific and targeted approaches to modulating miR-155 levels in the treatment of human disease.

There has been much consideration for using miR-155 as a biomarker of disease type and severity in human cancers where it is commonly overexpressed. Several instances of increased miR-155 levels correlating with more aggressive tumors with poor clinical outcomes have been reported (Chang et al., 2011; Han et al., 2012). However, a recent study looking at human melanoma patients found that increased miR-155 expression correlated with an improved prognosis (Segura et al., 2010). Although the study did not analyze distinct cellular subsets within the tumor, one could speculate that the increased miR-155 expression was a consequence of enhanced accumulation of immune cells within the tumor. Based upon our results here, it may prove valuable to carefully assess whether overexpression of miR-155 is occurring in tumor cells or in TILs that are actively fighting the tumor. This may give a more accurate assessment of whether increases in miR-155 are protective or deleterious.

While miR-155 plays a host protective role against solid tumor growth, miR-146a appears to limit immunity against the same tumor type. We provide evidence that these contrasting roles are the consequence of reciprocal effects by these miRNAs on the tumor accumulation of IFNγ expressing cells, including CD4+ and CD8+ T lymphocytes, which are critical mediators of antitumor immunity. These findings demonstrate that miRNAs in the immune system can play opposing roles in the regulation of a given phenotype. Thus, it is plausible that sets of miRNAs have evolved to provide balance to specific aspects of mammalian immunity, as has been proposed in stem cells (Melton et al., 2010). Consequently, we tested whether miR-155 and miR-146a function to provide immunological balance, or if one of these miRNAs has a dominant effect on IFNγ+ T cell formation and antitumor immunity. Using DKO mice, we determined that loss of miR-155 is largely epistatic to a deficiency in miR-146a in the contexts of IFNγ+ T cell formation and antitumor immunity. The enhanced antitumor responses observed in *miR-146a*−/− mice was not only dependent upon miR-155, but it was worse than that observed in Wt mice when miR-155 was also genetically absent. Therefore, our results indicate that miR-155 plays a dominant role, compared to miR-146a, in this context.

While studies carried out by our lab and others have provided evidence that these miRNAs oppose one another within T cells, it is also likely that miR-155 and miR-146a impact antitumor immune responses by also acting in non-T cell types, such as macrophages, dendritic cells and NK cells, where they have been shown to be expressed and to impact inflammatory responses (Boldin et al., 2011a; Cubillos-Ruiz et al., 2012; O'Connell et al., 2007; Trotta et al., 2012). Once conditional knockout mice are available for miR-155 and miR-146a then studies can be carried out to specifically test the relative contributions of these miRNAs to the functions of distinct cell types that drive tumor immunity, and this will shed additional light on the cellular basis of the observed epistasis.

In an effort to unravel the molecular basis for miR-155's function in the T cell compartment, we found the miR-155 target Ship1 to be part of the connection between miR-155 and IFNγ expression in CD4+ T cells. Ship1 is a phosphatase that negatively regulates cytokine signaling via repression of the PI3K pathway (Kerr, 2011). A recent study looking at deletion of Ship1 specifically in CD4+ T cells using a CD4-CRE mouse strain with floxed Ship1 alleles found that Ship1 expression in T cells promotes IFNγ expression by CD4+ T cells (Tarasenko et al., 2007). Consistent with these observations, our Ship1 shRNA experiments found that defective expression of IFNγ by *miR-155*−/− CD4+ T cells could be partially complemented by reducing levels of Ship1, which are elevated in these cells. The same observations were made in DKO CD4+ T cells indicating that Ship1 plays an increased inhibitory role when miR-155 is absent from either Wt or normally hyperactive *miR-146a*−/− T cells. This effect of Ship1 provides at least some of the explanation for why miR-155 is dominant in the CD4+ T cell compartment. However, miR-155 is known to repress a variety of different mRNA targets, such as cMaf, PI3K p85 and Socs1, which could also influence IFNγ responses by T cells. These proteins, in addition to Ship1, can act as inhibitors of IFNγ or cellular activation in general (Huang et al., 2012; Lu et al., 2009; Rodriguez et al., 2007). Therefore, it is likely that miR-155 repression of this group of targets underlies its function in CD4+ T cells. In the case of CD8+ T cells, we also observed increased Ship1 expression in the absence of miR-155. Ship1 has been shown to inhibit CD8+ T cell cytotoxicity (Tarasenko et al., 2007), suggesting that its regulation by miR-155 is also relevant in this cellular compartment. However, like CD4+ T cells, additional targets of miR-155 are also likely involved.

There is increasing evidence that the crosstalk between the pathways regulated by miR-155 and miR-146a in T cells involves regulators of NF-kB activity, a transcription factor involved in IFNγ transcription. *miR-146a*−/− T cells have just been shown to have increased activation of NF-kB following TCR engagement as a result of derepression of its targets IRAK1 and TRAF6 (Yang et al., 2012). This causes increased expression of IFNγ by effector T cells deficient in miR-146a. Consequently, it is possible that the elevated levels of Ship1 (Figure 5) and Socs1 (Lu et al., 2009) that are observed in *miR-155*−/− T cells act to inhibit NF-kB activation, as they have been shown to do in other cell types (Gabhann et al., 2010; Serezani et al., 2011; Strebovsky et al., 2011). This would negate the enhanced T cell activation observed in the absence of miR-146a alone. A careful dissection of these signaling pathways in the context of the different miRNA deficiencies will be an important future endeavor.

Taken together, our study identifies a protective role for miR-155, and an inhibitory function for miR-146a, during antitumor immune responses, and argues for the importance of developing highly specific methods of modulating miRNAs when such approaches are used to combat cancer or autoimmunity. Additionally, by combining approaches that enhance miR-155 and/or repress miR-146a levels in T lymphocytes with tumor vaccines or adoptive cell transfer therapies, one might achieve increased therapeutic efficacy in the clinic. Further studies will also be necessary to determine if miR-155 or miR-146a impact tumor metastasis

in addition to modulating tumor growth. Finally, the importance of miR-155 in regulating IFNγ+ T cell responses during tumor immunity is highlighted by the finding that a miR-155 deficiency is epistatic to a loss of miR-146a in this cellular compartment.

## EXPERIMENTAL PROCEDURES

### Mice

All mice were on a C57BL6 genetic background and housed in the animal facility at the University of Utah. Experiments were approved by the IACUC at the University of Utah and used mice 6-12 weeks of age. *miR-155*−/− were crossed with *miR-146a*−/− to create *miR-155*−/−*miR146a*−/− (DKO) mice. Genotyping was performed as described (Boldin et al., 2011b; Rodriguez et al., 2007). Xenogen live animal imaging to observe tumor expression of luciferase was performed as described (O'Connell et al., 2010a). Irradiation was delivered using an X-ray source.

### Tumor challenges and harvests

To create syngeneic subcutaneous tumors in mice, either EL4-luc lymphoma, B16-F10 melanoma, or B16-F1 melanoma cells were injected into the rear flanks of mice. The sites of tumor cell administration were shaved and cleaned before injection. Tumor growth was monitored over a time course by measuring tumor diameter. For analyses at the end of the time course, mice were euthanized and their tumors, spleens, and lymph nodes were removed and processed for FACS or histology. Following dissection, the tumors were weighed, minced into small pieces using a razor blade and subsequently digested using Accumax. After the enzymatic digestion, the tumor cells were washed before further analysis. In some experiments TILs were purified using FACS.

### Adoptive transfer of CD4+ and CD8+ T cells

For T cell transfer experiments, CD4+ or CD8+ T cells were purified from naïve mice (see below) and the indicated amounts of T cells were injected i.v. into recipient mice one day before tumor administration. In some experiments, recipients were first irradiated with 500 Rads using an X ray source before receiving T cells. To distinguish between donor and recipient T cells, CD45.1 and CD45.2 congenic mouse strains were used when possible.

### T cell isolation and retroviral infections

T cells were purified from RBC-lysed splenocytes using the MACS CD4+ or CD8+ T cell isolation kit (negative selection) from Miltenyi. Purity was assessed by FACS and routinely reached 90-95%. To create replication deficient MSCV-based retroviral particles carrying the Ship1 or a scrambled control sequence, 293T cells were transfected with the MGP backbone and pCL-Eco packaging plasmids and retrovector-containing supernatant was recovered after 48 hours. The shRNA Ship1 expression vector has been described previously (O'Connell et al., 2009). For retroviral transduction of CD4+ T cells, the cells were stimulated with αCD3 (3ug/ml) and αCD28 (2ug/ml) for 24 hours, subjected to a spin infection using retrovirus medium at 2500 RPMs and 30 C for 1.5 hours, then brought up in fresh activation medium for another 72 hours. Cellular infection was determined by microscopy or FACS to identify GFP+ cells.

### Intracellular staining and FACS

Intracellular staining was performed as described previously (O'Connell et al., 2010b). In short, $1\times10^6$ splenocytes, lymph node cells, or tumor suspension cells were restimulated with PMA and Ionomycin for 4 hours in the presence of Golgi Plug. Cells were next surface stained with αCD4 or αCD8 antibodies, washed, and permeabilized overnight using Perm

Fix. After washing with Perm Buffer, the cells were stained using a PE conjugated anti-mouse IFNγ antibody. Following washing, cells were analyzed by FACS using a BD LSR Fortessa. For FACS sorting, cells were surface stained with αCD45 (pan), αCD3, and αCD4 or αCD8 fluorophore-conjugated antibodies and cellular populations were sorted using a FACS Aria II in the FACS Core Facility at the University of Utah. Other antibodies used for FACS include αCD45.1 and αCD45.2.

### Western blotting, ELISA and qPCR

Western blotting using cellular extracts from T lymphocytes was performed using standard protocols. Antibodies against mouse Ship1 and β-Actin were obtained from Santa Cruz Biotechnology. For qPCR, RNA was extracted using the RNeasy or miRNeasy kits from Qiagen per manufacturer's instructions. Following cDNA synthesis using total RNA, SYBRgreen-based qPCR was performed with gene specific primers and the Roche Light Cycler 480. Primer sequences are available upon request. For detection of mature miRNAs 155 and 146a, or 5s ribosomal RNA, reagents and protocols from Exiqon were utilized. The ELISA assay used to quantify mouse IFNγ concentrations was obtained from eBioscience and performed using the manufacturer's suggested protocol.

### Histopathology

The tumors were dissected from the respective hosts and fixed with 10% formalin for at least 48 hours at room temperature. After fixation, the tumors were bisected across a maximum dimension and processed for paraffin embedding. 5 mm thick tissue sections were cut from paraffin blocks and stained with haematoxylin and eosin per standard H&E protocol. The histopathological analysis was performed by a board-certified pathologist, and the images were taken using Olympus BX41/DP72 microscope/camera. The magnification of the objective lens for each image is provided in the figures.

### Statistical Analysis

A Student's t-test was performed to determine statistical significance.

## Supplementary Material

Refer to Web version on PubMed Central for supplementary material.

## Acknowledgments

We would like to thank Allan Bradley for generously providing *miR-155*−/− mice, Lili Yang for providing the EL4-luc cells, and Glenn Dranoff for the B16-F10 cells. R.M.O. is supported by the NIH grant 5R00HL102228-04.

## Abbreviations

| | |
|---|---|
| **DKO** | Double knockout mice |
| **miRNA** | MicroRNA |

## REFERENCES

Bakirtzi K, Hatziapostolou M, Karagiannides I, Polytarchou C, Jaeger S, Iliopoulos D, Pothoulakis C. Neurotensin signaling activates microRNAs-21 and -155 and Akt, promotes tumor growth in mice, and is increased in human colon tumors. Gastroenterology. 2011; 141:1749–1761. e1741. [PubMed: 21806946]

Boldin MP, Taganov KD, Rao DS, Yang L, Zhao JL, Kalwani M, Garcia-Flores Y, Luong M, Devrekanli A, Xu J, et al. miR-146a is a significant brake on autoimmunity, myeloproliferation, and cancer in mice. J Exp Med. 2011a; 208:1189–1201. [PubMed: 21555486]

Boldin MP, Taganov KD, Rao DS, Yang L, Zhao JL, Kalwani M, Garcia-Flores Y, Luong M, Devrekanli A, Xu J, et al. miR-146a is a significant brake on autoimmunity, myeloproliferation, and cancer in mice. J Exp Med. 2011b

Chang S, Wang RH, Akagi K, Kim KA, Martin BK, Cavallone L, Haines DC, Basik M, Mai P, Poggi E, et al. Tumor suppressor BRCA1 epigenetically controls oncogenic microRNA-155. Nat Med. 2011; 17:1275–1282. [PubMed: 21946536]

Cubillos-Ruiz JR, Baird JR, Tesone AJ, Rutkowski MR, Scarlett UK, Camposeco-Jacobs AL, Anadon-Arnillas J, Harwood NM, Korc M, Fiering SN, et al. Reprogramming tumor-associated dendritic cells in vivo using miRNA mimetics triggers protective immunity against ovarian cancer. Cancer Res. 2012; 72:1683–1693. [PubMed: 22307839]

Dougan M, Dranoff G. Inciting inflammation: the RAGE about tumor promotion. J Exp Med. 2008; 205:267–270. [PubMed: 18268042]

Dunn GP, Old LJ, Schreiber RD. The immunobiology of cancer immunosurveillance and immunoediting. Immunity. 2004; 21:137–148. [PubMed: 15308095]

Filipowicz W, Bhattacharyya SN, Sonenberg N. Mechanisms of post-transcriptional regulation by microRNAs: are the answers in sight? Nat Rev Genet. 2008; 9:102–114. [PubMed: 18197166]

Gabhann JN, Higgs R, Brennan K, Thomas W, Damen JE, Ben Larbi N, Krystal G, Jefferies CA. Absence of SHIP-1 results in constitutive phosphorylation of tank-binding kinase 1 and enhanced TLR3-dependent IFN-beta production. J Immunol. 2010; 184:2314–2320. [PubMed: 20100929]

Haasch D, Chen YW, Reilly RM, Chiou XG, Koterski S, Smith ML, Kroeger P, McWeeny K, Halbert DN, Mollison KW, et al. T cell activation induces a noncoding RNA transcript sensitive to inhibition by immunosuppressant drugs and encoded by the proto-oncogene, BIC. Cell Immunol. 2002; 217:78–86. [PubMed: 12426003]

Han ZB, Chen HY, Fan JW, Wu JY, Tang HM, Peng ZH. Up-regulation of microRNA-155 promotes cancer cell invasion and predicts poor survival of hepatocellular carcinoma following liver transplantation. J Cancer Res Clin Oncol. 2012; 138:153–161. [PubMed: 22071603]

Huang X, Shen Y, Liu M, Bi C, Jiang C, Iqbal J, McKeithan TW, Chan WC, Ding SJ, Fu K. Quantitative proteomics reveals that miR-155 Regulates the PI3K-AKT pathway in diffuse large B-cell lymphoma. Am J Pathol. 2012; 181:26–33. [PubMed: 22609116]

Ikeda H, Old LJ, Schreiber RD. The roles of IFN gamma in protection against tumor development and cancer immunoediting. Cytokine Growth Factor Rev. 2002; 13:95–109. [PubMed: 11900986]

Jiang S, Li C, Olive V, Lykken E, Feng F, Sevilla J, Wan Y, He L, Li QJ. Molecular dissection of the miR-17-92 cluster's critical dual roles in promoting Th1 responses and preventing inducible Treg differentiation. Blood. 2011; 118:5487–5497. [PubMed: 21972292]

Kerr WG. Inhibitor and activator: dual functions for SHIP in immunity and cancer. Ann N Y Acad Sci. 2011; 1217:1–17. [PubMed: 21155837]

Lu LF, Boldin MP, Chaudhry A, Lin LL, Taganov KD, Hanada T, Yoshimura A, Baltimore D, Rudensky AY. Function of miR-146a in controlling Treg cell-mediated regulation of Th1 responses. Cell. 2010; 142:914–929. [PubMed: 20850013]

Lu LF, Thai TH, Calado DP, Chaudhry A, Kubo M, Tanaka K, Loeb GB, Lee H, Yoshimura A, Rajewsky K, Rudensky AY. Foxp3-dependent microRNA155 confers competitive fitness to regulatory T cells by targeting SOCS1 protein. Immunity. 2009; 30:80–91. [PubMed: 19144316]

Maekawa R, Kitagawa T, Hojo K, Wada T, Sato K. Distinct antitumor mechanisms of recombinant murine interferon-gamma against two murine tumor models. J Interferon Res. 1988; 8:227–239. [PubMed: 3132513]

Melton C, Judson RL, Blelloch R. Opposing microRNA families regulate self-renewal in mouse embryonic stem cells. Nature. 2010; 464:126.

Muranski P, Borman ZA, Kerkar SP, Klebanoff CA, Ji Y, Sanchez-Perez L, Sukumar M, Reger RN, Yu Z, Kern SJ, et al. Th17 cells are long lived and retain a stem cell-like molecular signature. Immunity. 2011; 35:972–985. [PubMed: 22177921]

Murugaiyan G, Beynon V, Mittal A, Joller N, Weiner HL. Silencing microRNA-155 ameliorates experimental autoimmune encephalomyelitis. J Immunol. 2011; 187:2213–2221. [PubMed: 21788439]

O'Connell RM, Balazs AB, Rao DS, Kivork C, Yang L, Baltimore D. Lentiviral vector delivery of human interleukin-7 (hIL-7) to human immune system (HIS) mice expands T lymphocyte populations. PLoS One. 2010a; 5:e12009. [PubMed: 20700454]

O'Connell RM, Chaudhuri AA, Rao DS, Baltimore D. Inositol phosphatase SHIP1 is a primary target of miR-155. Proc Natl Acad Sci U S A. 2009; 106:7113–7118. [PubMed: 19359473]

O'Connell RM, Kahn D, Gibson WS, Round JL, Scholz RL, Chaudhuri AA, Kahn ME, Rao DS, Baltimore D. MicroRNA-155 promotes autoimmune inflammation by enhancing inflammatory T cell development. Immunity. 2010b; 33:607–619. [PubMed: 20888269]

O'Connell RM, Rao DS, Chaudhuri AA, Baltimore D. Physiological and pathological roles for microRNAs in the immune system. Nat Rev Immunol. 2010c; 10:111–122. [PubMed: 20098459]

O'Connell RM, Taganov KD, Boldin MP, Cheng G, Baltimore D. MicroRNA-155 is induced during the macrophage inflammatory response. Proc Natl Acad Sci U S A. 2007; 104:1604–1609. [PubMed: 17242365]

Oertli M, Engler DB, Kohler E, Koch M, Meyer TF, Muller A. MicroRNA-155 Is Essential for the T Cell-Mediated Control of Helicobacter pylori Infection and for the Induction of Chronic Gastritis and Colitis. J Immunol. 2011

Philippidou D, Schmitt M, Moser D, Margue C, Nazarov PV, Muller A, Vallar L, Nashan D, Behrmann I, Kreis S. Signatures of microRNAs and selected microRNA target genes in human melanoma. Cancer Res. 2010; 70:4163–4173. [PubMed: 20442294]

Rodriguez A, Vigorito E, Clare S, Warren MV, Couttet P, Soond DR, van Dongen S, Grocock RJ, Das PP, Miska EA, et al. Requirement of bic/microRNA-155 for normal immune function. Science. 2007; 316:608–611. [PubMed: 17463290]

Segura MF, Belitskaya-Levy I, Rose AE, Zakrzewski J, Gaziel A, Hanniford D, Darvishian F, Berman RS, Shapiro RL, Pavlick AC, et al. Melanoma MicroRNA signature predicts post-recurrence survival. Clin Cancer Res. 2010; 16:1577–1586. [PubMed: 20179230]

Serezani CH, Lewis C, Jancar S, Peters-Golden M. Leukotriene B4 amplifies NF-kappaB activation in mouse macrophages by reducing SOCS1 inhibition of MyD88 expression. J Clin Invest. 2011; 121:671–682. [PubMed: 21206089]

Shiao SL, Ganesan AP, Rugo HS, Coussens LM. Immune microenvironments in solid tumors: new targets for therapy. Genes Dev. 2011; 25:2559–2572. [PubMed: 22190457]

Strebovsky J, Walker P, Lang R, Dalpke AH. Suppressor of cytokine signaling 1 (SOCS1) limits NFkappaB signaling by decreasing p65 stability within the cell nucleus. Faseb J. 2011; 25:863–874. [PubMed: 21084693]

Taganov KD, Boldin MP, Chang KJ, Baltimore D. NF-kappaB-dependent induction of microRNA miR-146, an inhibitor targeted to signaling proteins of innate immune responses. Proc Natl Acad Sci U S A. 2006; 103:12481–12486. [PubMed: 16885212]

Tarasenko T, Kole HK, Chi AW, Mentink-Kane MM, Wynn TA, Bolland S. T cell-specific deletion of the inositol phosphatase SHIP reveals its role in regulating Th1/Th2 and cytotoxic responses. Proc Natl Acad Sci U S A. 2007; 104:11382–11387. [PubMed: 17585010]

Thai TH, Calado DP, Casola S, Ansel KM, Xiao C, Xue Y, Murphy A, Frendewey D, Valenzuela D, Kutok JL, et al. Regulation of the germinal center response by microRNA-155. Science. 2007; 316:604–608. [PubMed: 17463289]

Trotta R, Chen L, Ciarlariello D, Josyula S, Mao C, Costinean S, Yu L, Butchar JP, Tridandapani S, Croce CM, Caligiuri MA. miR-155 regulates IFN-gamma production in natural killer cells. Blood. 2012; 119:3478–3485. [PubMed: 22378844]

Volinia S, Calin GA, Liu CG, Ambs S, Cimmino A, Petrocca F, Visone R, Iorio M, Roldo C, Ferracin M, et al. A microRNA expression signature of human solid tumors defines cancer gene targets. Proc Natl Acad Sci U S A. 2006; 103:2257–2261. [PubMed: 16461460]

Yang L, Boldin MP, Yu Y, Liu CS, Ea CK, Ramakrishnan P, Taganov KD, Zhao JL, Baltimore D. miR-146a controls the resolution of T cell responses in mice. J Exp Med. 2012

Yim JH, Wu SJ, Lowney JK, Vander Velde TL, Doherty GM. Enhancing in vivo tumorigenicity of B16 melanoma by overexpressing interferon regulatory factor-2: resistance to endogenous IFN-gamma. J Interferon Cytokine Res. 1999; 19:723–729. [PubMed: 10454342]

Zhao JL, Rao DS, Boldin MP, Taganov KD, O'Connell RM, Baltimore D. NF-{kappa}B dysregulation in microRNA-146a-deficient mice drives the development of myeloid malignancies. Proc Natl Acad Sci U S A. 2011

Zheng SR, Guo GL, Zhang W, Huang GL, Hu XQ, Zhu J, Huang QD, You J, Zhang XH. Clinical significance of miR-155 expression in breast cancer and effects of miR-155 ASO on cell viability and apoptosis. Oncol Rep. 2012; 27:1149–1155. [PubMed: 22245916]

Zitvogel L, Tesniere A, Kroemer G. Cancer despite immunosurveillance: immunoselection and immunosubversion. Nat Rev Immunol. 2006; 6:715–727. [PubMed: 16977338]

## Highlights

- miR-155 promotes and miR-146a inhibits both CD4+ and CD8+ T cell antitumor responses
- DKO mice reveal epistasis between miR-155 and miR-146a during tumor immunity
- miR-155 regulation of IFNγ involves repression of its target Ship1 in T cells

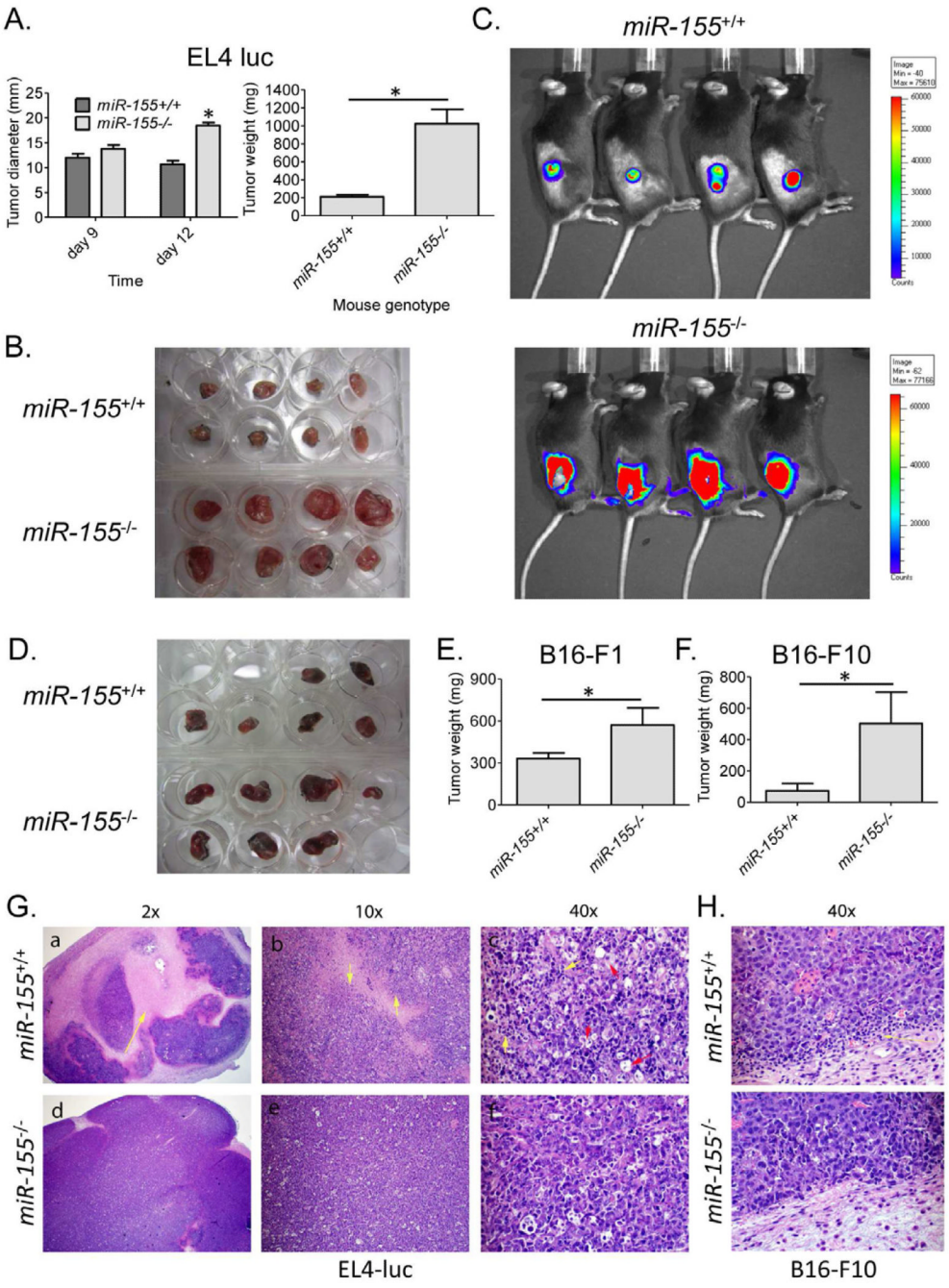


**Figure 1. Enhanced solid tumor growth in *miR-155*−/− mice**

**(A)** Wt and *miR-155*−/− mice were administered $2\times10^6$ EL4-luc cells subcutaneously in their rear flanks and tumor growth was monitored over time (n=8). Tumor diameters and weights after 12 days are shown. **(B)** Tumors dissected from the mice in **A**. **(C)** Live animal imaging was performed to detect tumor expression of luciferase. **(D)** Wt and *miR-155*−/− mice were challenged with $1\times10^6$ B16-F1 cells and their growth was followed for 14 days. The dissected tumors from the groups are shown. **(E)** Tumor weights from **D**, or **(F)** from mice given $5\times10^5$ B16-F10 melanoma cells for 19 days are shown (n=5-7). **(G)** H&E stained EL4-luc, or **(H)** B16-F10, tumor sections from Wt or *miR-155*−/− mice shown at the

indicated magnifications. * denotes a p value less than 0.05. Data are presented as +/− SEM. In the 2x and 10x images the yellow arrows indicate necrosis. In the 40x picture, the yellow arrows indicate TILs and the red arrows indicate macrophages. See also Figure S1.

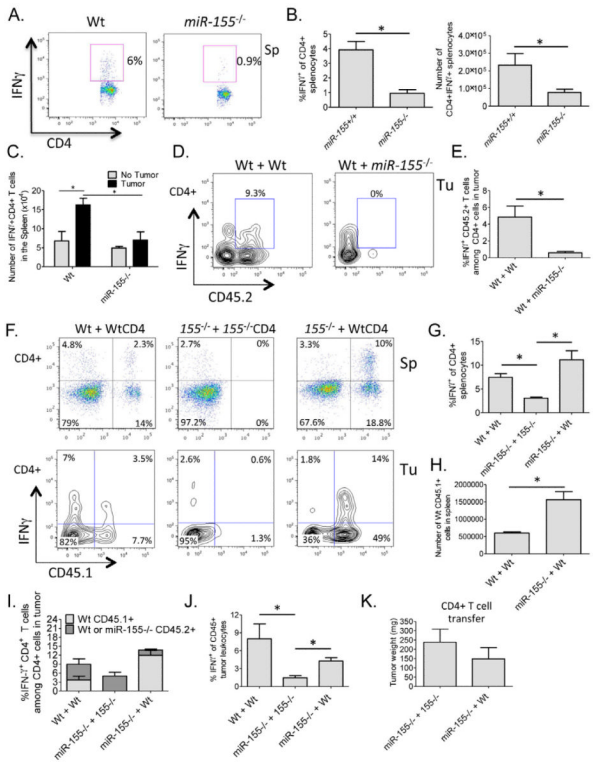


**Figure 2. miR-155 promotes IFNγ+CD4+ T cell formation in tumor bearing mice through a CD4+ T cell intrinsic mechanism**

**(A)** IFNγ expression by CD4+ T cells from the spleens of EL4-luc tumor bearing Wt or *miR-155*−/− mice following 12 days of tumor growth. **(B)** Results from **A** are shown graphically for multiple mice (n=5). **(C)** Number of IFNγ+CD4+ T cells in the spleens of Wt or *miR-155*−/− mice with and without B16-F10 tumors for 14 days. **(D)** FACS plots (gated on CD4+ T cells) showing IFNγ expression by transferred Wt or *miR-155*−/− CD45.2+ CD4+ T cells in the tumors of Wt CD45.1+ B16-F10 tumor bearing mice. **(E)** Graphs from multiple mice in **D** (n=5). **(F)** FACS plots showing IFNγ expression by transferred Wt CD45.1+ CD4+ T cells in the spleens (top) or tumors (bottom) of Wt or *miR-155*−/− CD45.2+ B16-F10 tumor bearing mice. Note: transferred *miR-155*−/− CD4+ cells are CD45.2+ and all plots are gated on CD4+ T cells. **(G)** Graph showing IFNγ expression by the splenic CD4+ T cell compartment in B16-F10 tumor bearing *miR-155*−/− mice receiving Wt CD4+ T cells (n=5-7). **(H)** Total number of engrafting CD45.1+ Wt CD4+ T cells in Wt versus *miR-155*−/− tumor bearing mouse spleens. **(I)** Graph showing the percentage of IFNγ+CD4+ T cells among total CD4+ T cells in the tumor. Contribution by transferred vs. endogenous cells is also shown. **(J)** The amount of IFNγ-expressing CD45+ cells among total CD45+ cells in the B16-F10 tumors is shown graphically for multiple mice of the indicated genotypes (n=5-7). **(K)** Tumor weights from **J**. * denotes a p value less than 0.05. Data are presented as +/− SEM. Tu - tumor, Sp - spleen. See also Figures S2 and S3.

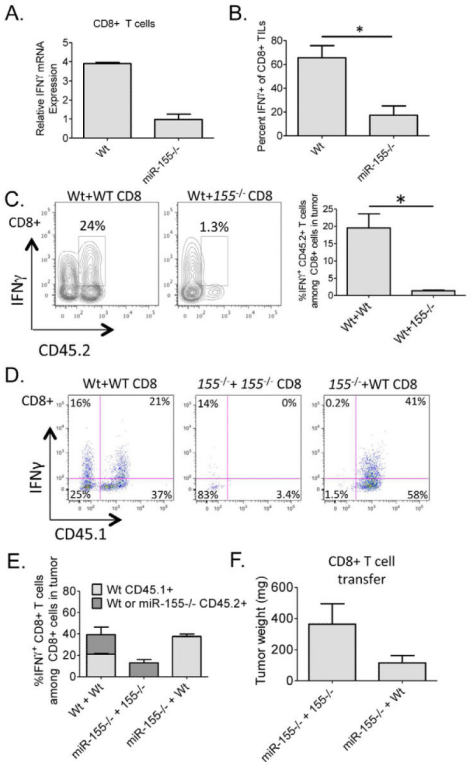


**Figure 3. miR-155 promotes IFNγ+CD8+ T cell responses in tumor bearing mice through a CD8+ T cell intrinsic mechanism**

**(A)** Expression levels of IFNγ in αCD3 and αCD28 activated CD8+ splenic T cells from Wt or *miR-155*−/− mice were assayed by qPCR. **(B)** The percentage of IFNγ+CD8+ TILs among total CD8+ TILs from tumors growing in Wt or *miR-155*−/− mice (n=5). **(C)** FACS plots of B16-F10 tumor cell suspensions looking at IFNγ expression by the transferred Wt and miR-155−/− CD45.2+ CD8+ T cells in CD45.1 Wt tumor bearing hosts (n=5). Plots are gated on CD8+ T cells. **(D)** FACS plots of B16-F10 tumor cell suspensions looking at IFNγ expression by the transferred Wt CD45.1+ CD8+ T cells in Wt or *miR-155*−/− CD45.2+ tumor hosts. Plots are gated on CD8+ T cells. **(E)** The percentage of CD45.2+ endogenous CD8+ TILs versus transferred Wt CD45.1+ CD8+ TILs expressing IFNγ among total CD8+ T cells is shown graphically for multiple mice of the indicated genotypes (n=5-7). **(F)** Tumor weights from **D** are shown. * denotes a p value less than 0.05. Data are presented as +/− SEM.

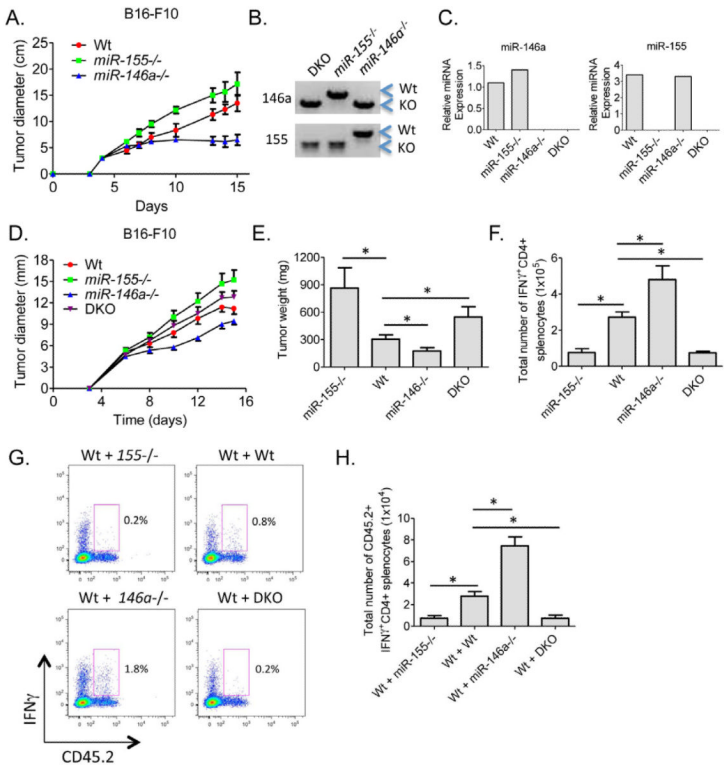


**Figure 4. Enhanced tumor growth and defective numbers of IFNγ-expressing CD4+ T cells in *miR-155*−/− *miR-146a*−/− DKO mice**

**(A)** Wt, *miR-155*−/− and *miR-146a*−/− mice were inoculated subcutaneously with $1\times10^6$ B16-F10 tumor cells and the tumor diameters were measured over a 15-day time course (n=5). **(B)** Genotyping results from PCR assays demonstrating the generation of miR-155 and miR146a double knockout (DKO) mice. **(C)** Expression of miR-155 or miR-146a in activated CD4+ T cells from the indicated genotypes. **(D)** B16-F10 tumor growth in Wt, *miR-155*−/−, *miR-146a*−/− and DKO mice (n=10). **(E)** Tumor weights following resection 15 days after tumor cell injection (n=15-24). **(F)** Total number of IFNγ+CD4+ T cells in the spleens of Wt, *miR-155*−/−, *miR-146a*−/− and DKO tumor bearing mice (n=5). **(G)** CD45.2+ Wt, *miR-155*−/−, *miR-146a*−/− or DKO naïve CD4+ T cells were injected into sub-lethally irradiated CD45.1+ Wt mice one day before being inoculated with $5\times10^5$ B16-F10 cells. IFNγ expression by the transferred CD4+ T cells in the spleens of tumor bearing mice was assayed 15 days later. **(H)** Number of IFNγ expressing cells from **G** is shown (n=5). * denotes a p value less than 0.06. Data are presented as +/− SEM.

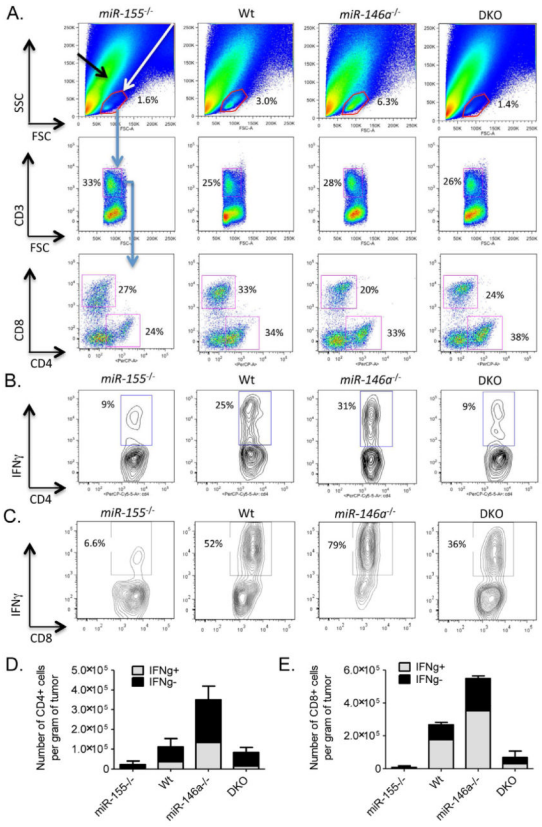


**Figure 5. Dominant role for miR-155 versus miR-146a during T cell-mediated antitumor immune responses**

**(A)** Representative FACS plots showing the percentage of tumor infiltrating CD3+CD4+ and CD3+CD8+ TILs in Wt, *miR-155*−/−, *miR-146a*−/− and DKO mice (n=5). Representative FACS plot demonstrating expression of IFNγ by **(B)** CD4+ and **(C)** CD8+ TILs from the indicated genotypes (n=5). The number (per gram of tumor) of IFNγ+ and IFNγ- **(D)** CD3+CD4+ or **(E)** CD3+CD8+ TILs sorted from tumors growing in the different genotypes is shown. Data represent two independent experiments. Data are presented as +/− SEM. See also Figure S4.

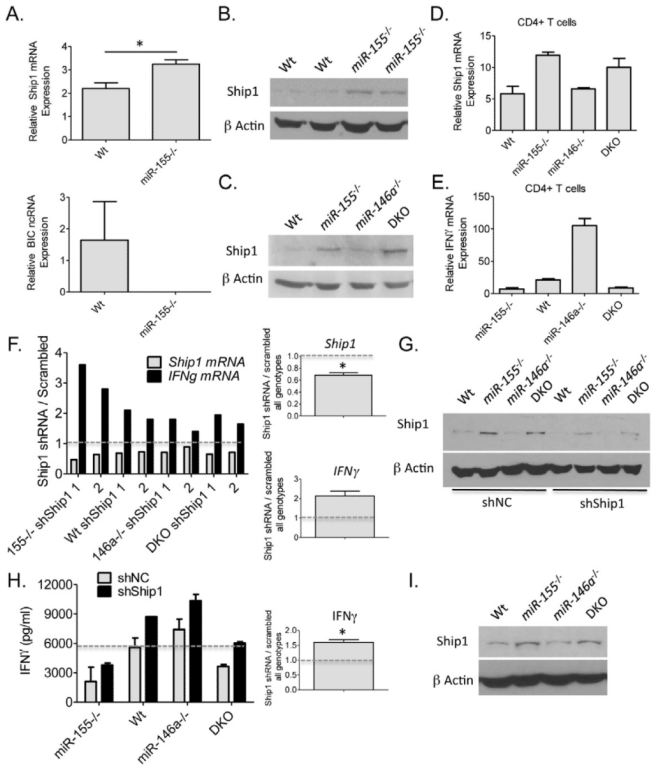


**Figure 6. Ship1 is a target of miR-155 in T lymphocytes**

**(A)** Expression levels of Ship1 mRNA and BIC ncRNA were determined in CD4+ T cells purified from the spleens of tumor bearing mice Wt and *miR-155*−/− mice (n=4). **(B)** Expression of Ship1 was quantified in activated Wt and *miR-155*−/− CD4+ T cells by Western blotting. Data from two Wt and two *miR-155*−/− mouse T cell donors are shown. **(C)** and **(D)** Expression of Ship1 in αCD3 and αCD28 activated CD4+ splenic T cells from Wt, *miR-155*−/−, *miR-146a*−/− and DKO mice was assayed by Western blotting and qPCR. **(E)** Expression of IFNγ mRNA in the same cells from **D** is shown (n=2). **(F)** αCD3 and αCD28 antibody activated CD4+ splenic T cells from Wt, *miR-155*−/−, *miR-146a*−/− and DKO mice were transduced with a control or one of two different Ship1 siRNA producing retroviral vectors after 24 hours of activation. Expression of *Ship1* and *IFNγ* mRNA levels were assayed by qPCR after 72 hours of knockdown. Data are presented as the ratio of expression in the siRNA vs. control (scrambled) conditions. The average knockdown of *Ship1* or increase in *IFNγ* for all genotypes is shown on the right. **(G)** Knockdown of Ship1 in the different cell types by the Ship1 shRNA was determined by Western blotting. **(H)** Retroviral transduction of shRNAs against Ship1 into CD4+ T cells from the indicated genotypes was performed as in **F**. IFNγ protein concentrations in the supernatants were determined by ELISA 72 hours after T cell activation. **(I)** Ship1 expression levels were determined by Western blotting in αCD3 and αCD28 activated CD8+ T cells from the indicated genotypes. Average increase in IFNγ for all genotypes is shown on the right. * denotes a p value less than 0.05. Data are presented as +/− SEM. See also Figures S5 and S6.